Acta Universitatis Sapientiae
Electrical and Mechanical Engineering, 11 (2019) 22-33

DOI: 10.2478/auseme-2019-0002

Detailed Model of a Common Rail Injector

Sándor VASS[1], Máté ZÖLDY[2]

[1] Department of Automotive Technologies, Faculty of Transportation Engineering and Vehicle Engineering, Budapest University of Technology and Economics, Budapest,
e-mail: sandor.vass@gjt.bme.hu
[2] Department of Automotive Technologies, Faculty of Transportation Engineering and Vehicle Engineering, Budapest University of Technology and Economics, Budapest,
e-mail: mate.zoldy@gjt.bme.hu

Manuscript received February 29, 2019; revised July 16, 2019

Abstract: This work is about the validation of a Common Rail (CR) injector model. The model describes injector internal behavior in a detailed way, validation is done using dosage measurements and needle lift traces.

The model contains fluid dynamic, mechanic and electro-magnetic parts describing all important internal processes. To compare the modelling results against measurement data, three test cases were chosen on a medium duty test engine to represent a wide range of operation points. Dosage measurements were done by averaging the injected mass of 1500 injections, each measurement repeated three times. Needle displacement was measured using an injector equipped with a needle lift sensor in the same operating points. The results of the simulated injector and the measured values showed good conformity both in needle displacement and injected fuel mass, so the model can be a basis for further injector and combustion analyses.

Keywords: Common Rail, injector, simulation, modelling, validation, internal combustion engines.

1. Introduction

Introduction of the Common Rail (CR) injection systems was one of the most important steps in injection developments. CR systems offer a flexibility in injection pressure, timing and length under any engine operating point [1]. CR systems separate the pressure generation physically from the fuel metering, eliminating injection pressure drop at low speeds and loads, a hallmark of conventional injection systems [2]. This flexibility, coupled with the possibility of cutting the injection into three to seven phases, allows more control over the combustion and exhaust after treatment processes, as they mostly depend on the air-fuel mixing and burning during and after the injection event. However, it is highly time and resource consuming to set up the system for all operating points of different engines. Controlling combustion is the best tool to minimise tail pipe emission that is one of the most neuralgic barriers of the utilisation of diesel engines [3,4].

It is challenging to measure the internal mechanisms of a CR injector, due to the high pressures, quick pressure changes, small chambers and holes, fast operation and high flow velocities. The best solution for these problems is to create a detailed model of the injector, where all hydraulic, mechanic and electromagnetic subsystems are represented, so the internal working conditions can be analysed in an economical and efficient manner.

As CR systems became more and more popular, CR injector models continuously appeared in literature more and more frequently. Some tried to model the whole injection system, including high pressure pump and rail pipes [5-6], making them very complex, but most works contained only the injector itself. Control oriented models with simplified structures were developed [7-8], but most of the papers describe injector operation in a detailed manner. However, the latter mostly included only mechanical and fluid dynamical parts [9-13]. Publications rarely contain the electromagnetic circuit of the solenoid, but the work of Bianchi et al. stands out [14-17], as a complete, detailed and validated CR injector. If the solenoid model is neglected, usually an interpolation of force data acting on the anchor is used instead [18-19].

Elastic axial deformation of the needle and control piston is taken into consideration in all works, along with the injector body if necessary [20]. This phenomenon affects the effective needle displacement and the needle-seat passage area at the orifice holes crucially, so it cannot be neglected.

An accurate fluid dynamic part is also a key factor of CR injector modelling. Cavitation is always a part of that, since it affects the discharge coefficient of the nozzle and other holes, and through this on the injected fuel mass. This is why much emphasize was put on determining and describing this phenomenon occurring in various hole geometries [21].

Based on the references listed above, a CR injector shall employ three main model types: an electrical, a hydraulic and a mechanical one. If the goal is to create an accurate and predictive injector model, all three of them have to be considered and simulation results shall be compared to measurement data. There can be several aspects of injector model validation, e.g. mechanical parts, fluid dynamic behavior, etc. In this paper the needle movement measurements will be used to validate the mechanical and electromagnetic systems, while the dosage measurements serve to validate the hydraulic description. These together describe injector operation comprehensively and if simulation results show good conformity with the measurement data, the model can be stated valid.

2. Injector model

The model described below was based upon a Bosch CRIN1 type injector for commercial vehicles. The description of the internal buildup and detailed working principles of the injector can be seen in [2].

A hybrid model containing electromagnetic, hydraulic and mechanical parts was built up in order to maintain accuracy and study of the injectors' internal processes. The structure was first presented in [22], and then validated against control piston lift measurements in [23], but dosage validation was needed to make it predictive.

The model was implemented in a commercial simulation software named GT-Suite, in the GT-Fuel submodule. It is capable of calculating problems in different disciplines of physics, i.e. it is capable of electromechanical, thermal, fluid-dynamical and mechanical simulations [24].

A. The mechanical model

Mass-spring-damper scheme was used to model the moving part of the injector. Masses in the simulation environment may translate with a given velocity in planar directions; equations are based on Newton's second law and calculated in every coordinate direction.

Viscous, elastic and body forces are also calculated during simulation, external forces can also be applied.

As *Fig. 1* shows, the injector needle in this model is handled as a rigid body, although the high working pressures of the injection system causes appreciable deformation of the parts. Modelling of this phenomenon has a critical importance on the accuracy of the simulation. To simulate the change of the actual needle stroke due to deformation, material stiffness and damping was reduced into one element, namely the control piston. The mass of the control piston was split into two parts with identical masses and connected by a spring and a damper element. These could be described as resultant stiffness and damping of the whole system, which could be defined using measurement results of the needle lift sensor and the line pressure sensor. As the needle lift sensor indicates the control piston stroke change due to deformation, the force acting on the piston can be obtained from the measured fuel pressure and the piston diameter. This method eliminates the laborious work of defining the stiffness of all different parts one by one and provides accurate results.

Evaluation of the damping factor is far more difficult, considering that the damping factor shall include elements not only by the internal friction, but also from fluid viscosity and friction between piston and liner. Experimental evidences show that the friction component of the damping is more important, but it cannot be evaluated theoretically, since machining tolerances affect it mostly. Therefore, damping must be estimated during the model tuning phase.

Masses of all parts were measured using a medical grade scale. Contact stiffnesses were estimated during the model tuning phase, here the main target was to adjust the bouncing of the needle, control piston and solenoid anchor according to other measurements in literature.

B. Hydraulic model

The hydraulic model strictly follows the system layout. This means that all volumes downstream the high pressure tubes coming from the rail, down to the nozzle holes are modelled, containing all internal flow passages defined with the exact geometries as they were manufactured. The rail tube and high pressure pump is replaced by an unsteady pressure boundary condition, which was measured in the rail tube during the injection event. Thus the hydraulic system of the injector has been modelled as a network of pipes and chambers connected by orifices, higher level components from the software model library were used to calculate hydraulic forces caused by fuel pressure and flow and fuel leakage is also modelled at the joint surfaces. Calculation is based on one-dimensional, unsteady, compressible flow and takes into consideration the dynamics of the attached mechanical components and structural heat transfer. *Fig. 1* and *Fig. 2* show the hydraulic and mechanical model parts of the injector. In *Fig. 1* the injector body is presented, while *Fig. 2* shows the assembly located in the solenoid.

The geometrical parameters needed in fluid-dynamic equations were measured and implemented in the model; the characteristics of the three main orifices can be followed in *Table 1*. The diameters of internal flow passages and pistons, chambers were measured using simple slide-gauge. Smaller holes i.e. A- and Z-throttles were measured with the help of a microscope and a microscope scale ruler. The geometry nozzle hole was defined by a destructive measurement method, where a similar nozzle body was cut through the axis of a nozzle hole, so the length, diameter and shape of the hole could be determined (*Fig. 3*).

Because pressure and temperature can remarkably vary in CR systems, it is important to have accurate properties of the medium. In these simulations ISO4113 test oil was used; density, dynamic viscosity and bulk modulus were given as functions of temperature and pressure.

Table. 1: Geometric parameters of orifices (Dh - diameter of hole, L – length of hole, r – inlet corner radius)

	D_h [μm]	L [mm]	r [μm]
Injector orifice hole	152	1	20
Hole A	268	0.6	65
Hole Z	220	0.47	55

C. Electromagnetic model

The electromagnetic model of the solenoid is responsible for transforming input current to mechanical force acting on the anchor mass through magnetic circuits. The electromagnetic force is considered by the mechanical model part and anchor dynamics are calculated according to its value. It is calculated based on the reluctance of the circuit: when current begins to flow in the coil, magnetic flux flows through the elements and electromagnetic force will be generated between the surfaces of the air gaps. A detailed explanation of the system and its working principles can be found in [25].

3. Results and discussion

A. Test bench layout

All measurements were realized using a four cylinder turbocharged Diesel engine installed on an engine test bench [26]. Due to the specific high pressure fuel connection of the CRIN1, an injector mount would be difficult to manufacture, so a cylinder head similar to the one on the engine was used to accommodate the injector (*Fig. 4*). One of the injectors on the engine was disconnected from the rail tube and the ECU. A flexible high pressure fuel hose was mounted between the rail and the injector fuel inlet, to provide fuel supply to the examined injector, thus the engine ran with three cylinders while the connections of the fourth drove the examined injector.

The tested injector was equipped with a needle lift sensor measuring control piston movement; a current clamp was used to record the driving current of the injector, while a line pressure sensor measured instantaneous rail pressure.

Different injection pressures and excitation times were reached by setting different engine operation points on the test bench in the most commonly used engine speed and load range.

Injections occurred in a measuring glass in order to measure the cumulated injected mass, from which the dosage could be calculated.

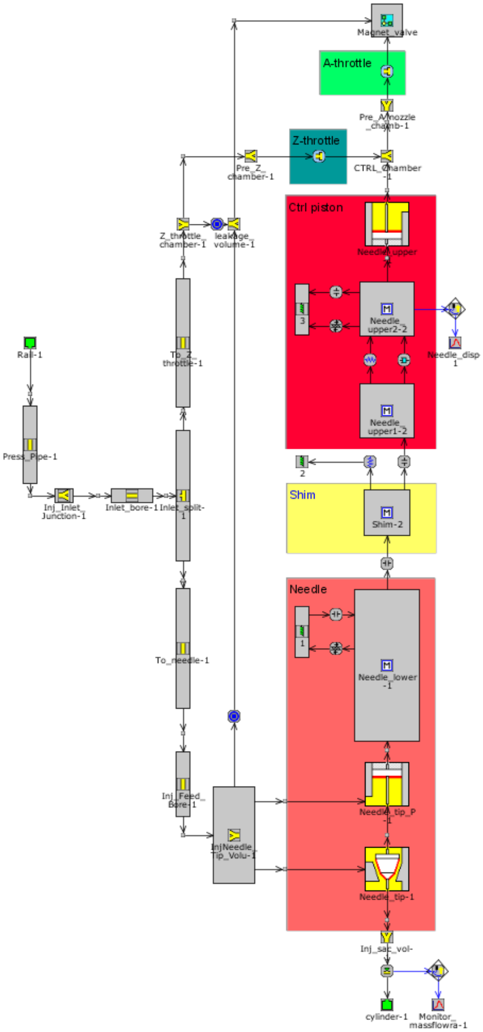

Figure 1: Hydraulic and mechanical models of the injector body.

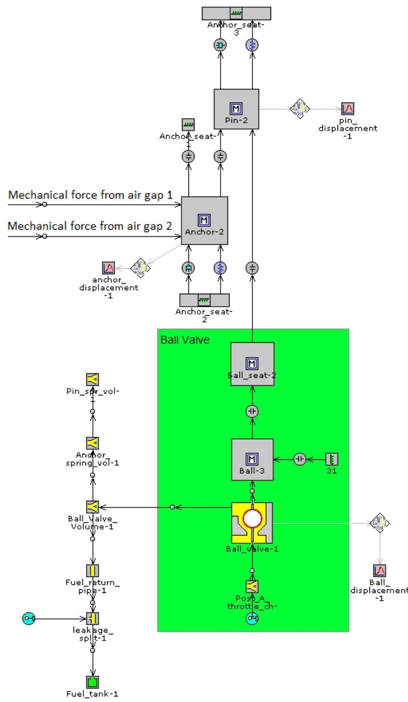

Figure 2: Hydraulic and mechanical models of the solenoid assembly.

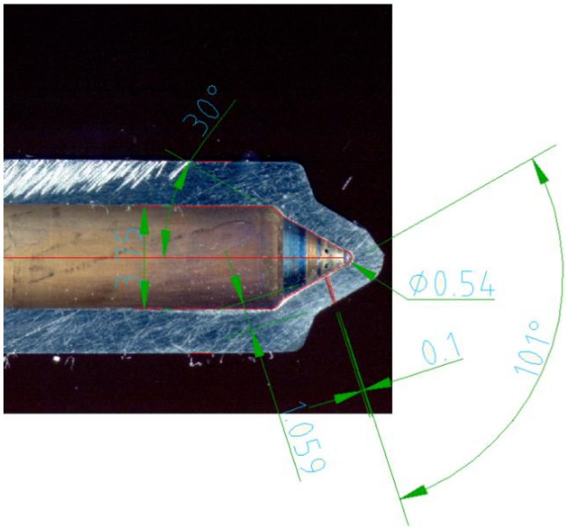

Figure 3: Geometry of the injector nozzle hole.

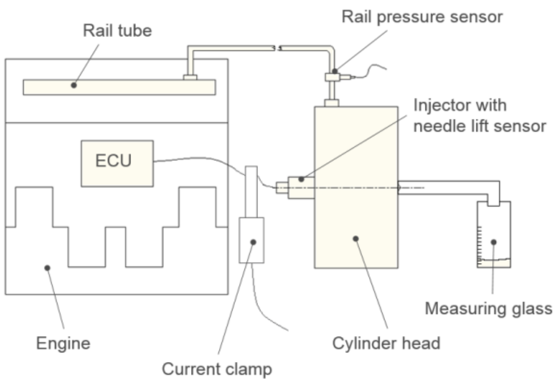

Figure 4: Test-bench layout.

B. Test cases and boundary conditions

Three different test cases are presented in this work with three different engine operating points. The engine speeds, loads and the corresponding measured injection pressures and excitation times can be followed in *Table 2*.

Table. 2: Test case parameters

Test case	Engine speed [Rpm]	Engine torque [Nm]	Injection pressure [bar]	Excitation time [ms]
1	1500	300	680	2.55
2	1500	200	540	1.9
3	1500	100	450	1.15

C. Validation and results

The model has been validated by comparison with measurements in terms of injector control piston lift and injected dosage. Needle lift could not be directly measured, the sensor recorded the control piston position. Dosage was calculated from the cumulated injected mass, derived from the number of injections.

Three experimental cases were studied with different rail pressures and opening times. All of the cases represent single injections without pre or post phases, because this particular engine does not use pilot or post injection in the main operation range. Control piston lifts of the three cases can be followed in *Fig. 5*.

The effect of axial deformation of the control piston and needle is obvious on these position traces. Case 1 has the largest stroke, because rail pressure is the highest here and along with rail pressure the axial force increases also. It is worth noticing that stroke difference reaches 20μm between cases 1 and 3. It is also worthwhile to point out the ‘humps’ at the beginning of every needle lift. This is caused by the sudden pressure drop when the ball valve opens the control chamber and the control piston expands axially before the actual movement begins.

All simulations follow the measured traces with good accuracy. To determine this accuracy, the root mean square (RMS) errors were calculated for every case based on the following equation:

$$\varepsilon_i = \sqrt{\frac{1}{T}\int_0^T \left(\frac{l_{i,meas}-l_{i,sim}}{l_{i,meas}}\right)^2} \qquad (1)$$

where:

ε_i - RMS error,

T - simulation time range,

$l_{i,meas}$ - measured control piston lift,

$l_{i,sim}$ - simulated control piston lift.

In all cases a certain amount of noise can be noticed, but it stays in a tolerable range, so no filtering was used. This way the time shift of the filter was avoided and more accurate results could be provided.

The RMS values are presented in *Table 3*. All RMS error values are less than 1%, so based on *Fig. 5* with the results shown in *Table 3*, it can be stated, that the simulation predicts the needle lifts of the injector accurately.

Dosage calculation was based on cumulative injected mass measurement. Measuring time was chosen to get a sufficiently large cumulated injected mass value and number of injections, this way measuring accuracy could be increased. All measurements were repeated three times. *Table 4* contains the measuring circumstances, measured and simulated dosage values.

Table 5 shows the absolute and relative deviations of the simulated dosage. Looking at the deviation values it can be clearly stated, that the model reproduces measured dosage accurately in the studied operating points. All deviation values are below or equal to 2%.

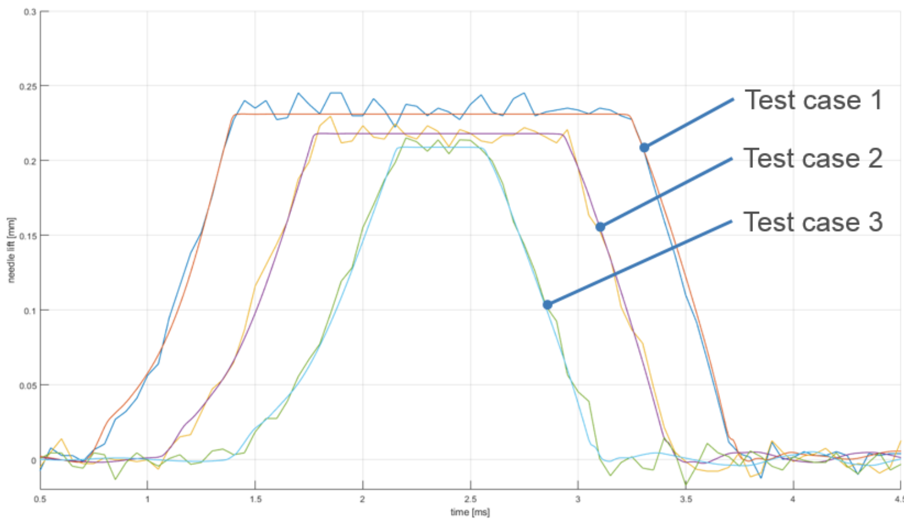

Figure 5: Measured and simulated control piston lifts for test cases 1 to 3.

Table. 3: RMS error of the needle lifts

Test case	RMS error
1	0.0054
2	0.0054
3	0.0054

Table. 4: Measured and simulated dosage

Test case No.	Measuring time [s]	Measured mass [g]	Number of injections [pcs]	Dosage [mg]	Simulated dosage [mg]
1	120	140,41	1500	93,60	91,38
2	120	90,32	1500	60,21	59,40
3	120	48,88	1500	32,59	33,25

Table. 5: Measured and simulated dosage deviation

Test case No.	Deviation [mg]	Deviation [%]
1	2,22	**2,03**
2	0,81	**0,48**
3	0,66	**0,22**

4. Conclusion

In this paper a detailed model of a CR injector for commercial vehicles was presented and validated against needle lift data and dosage values. Three test cases were chosen to represent operation points in the mostly used partial load range. The simulated control piston movement and injected mass accurately matched the measured curves and values in every test case.

The fluid dynamic and mechanic model parts were presented in details to investigate the working principles of the injector internal parts. Simulation validation against injection rate measurements shall be done in the future to make the model fully predictive.

References

[1] Strumpp, G., Ricco, M. “Common Rail – An Attractive Fuel Injection System for Passenger Car DI Diesel Engines”, *SAE Technical Paper Series* 960870, 1996.

[2] Zellbeck, H. and Schmidt G. “Einspritzsysteme für zukünftige Anforderungen an schnellaufenden Dieselmotor”, *MTZ*, vol. 56, no. 11, pp. 648-655, 1995.

[3] Tutak W, Jamrozik A, Bereczky Á and Lukács K. “Effects of injection timing of diesel fuel on performance and emission of dual fuel diesel engine powered by diesel/E85 fuels”, *TRANSPORT (VILNIUS)*, vol. 33, no. 3, pp. 633-646, 2018.

[4] Farkas, O., Szabados, G., Antal, Á. and Török, Á. “Experimental Investigation of Discoloration Generated by a CI ICE’s Exhaust Gas on Various Stone Types”, *Periodica Polytechnica Transportation Engineering*, vol. 46, no. 3, pp. 158-163. doi: https://doi.org/10.3311/PPtr.12120, 2018.

[5] Sabau, A., Barhalescu, M. and Oanta, E. “Modeling of high pressure fuel injection systems”, *Annals of DAAAM for 2012 & Proceedings of the 23rd International DAAAM Symposium*, vol. 23, no.1, 2011.

[6] Chiavola, O., Giulanelli, P. "Modeling and Simulation of Common rail Systems", *SAE Technical Paper Series*, 2001-01-3183, 2001.
[7] Lino, P., Maione, B. and Rizzo, A. "Nonlinear modelling and control of a common rail injection system for diesel engines", *Applied Mathematical Modeling*, vol. 31, pp. 1770-1784, 2007.
[8] Palamondon, E., Seers, P., "Development of a simplified dynamic model for a piezoelectric injector using multiple injection strategies with biodiesel / diesel-fuel blends", *Applied Energy*, no. 131, pp. 411-424, 2014.
[9] Brusca, S., Giuffrida, A., Lanzafame, R. and Corcione, G. E. "Theoretical and experimental analysis of diesel sprays behavior from multiple injections common rail systems", *SAE Technical Paper Series*, 2002-01-2777, 2002.
[10] Catalano, L. A., Tondolo, V. A. and Dadone, A. "Dynamic rise of pressure in the common rail fuel injection system", *SAE Technical Paper Series*, 2002-01-0210, 2002.
[11] Digesu, P., Ficarella, A., Laforgia, D., Bruni, G. and Ricco, M. "Diesel Electro-Injector: A Numerical Simulation Code", *SAE Technical Paper Series*, 940193, 1994.
[12] Mulemane, A., Han, J-S., Lu P-H., Yoon, S-J. and Lai, M-Ch. "Modeling Dynamic Behavior of Diesel Fuel Injection Systems", *SAE Technical Paper Series*, 2004-01-0536, 2004.
[13] Payri, R., Climent, H., Salvador, F. J. and Favennec, A. G. "Diesel injection system modelling. methodology and application for a first-generation common rail system", *Proceedings of the Institution of Mechanical Engineering*, vol. 218, part D, 2004.
[14] Bianchi, G. M., Pelloni, P., Corcione, E. and Luppino, F. "Numerical analysis of passenger car HSDI diesel engines with the 2nd generation of common rail injection systems: The effect of multiple injections on emissions", *SAE Technical Paper Series*, 2001-01-1068, 2001.
[15] Bianchi, G. M., Falfari, S., Pelloni P., Filicori, F. and Milani, M. "A Numerical and Experimental Study on the Possible Improvements of C.R. Injectors", *SAE Technical Paper Series*, 2002-01-0500, 2002.
[16] Bianchi, G. M., Falfari, S., Pelloni P., Kong, S-C. and Reitz, R.D. "Numerical Analysis of High Pressure Fast-Response C.R. Injector Dynamics", *SAE Technical Paper Series*, 2002-01-0213, 2002.
[17] Bianchi, G. M., Falfari, S., Parotto, M. and Osbat, G. "Advanced Modeling of Common Rail Injector Dinamics and Comparison with Experiments, *SAE Technical Paper Series*, 2003-01-0006, 2003.
[18] Amiola, V., Ficarella, A., Laforgia, D., De Matthaeis, S. and Genco, C. "A theoretical code to simulate the behavior of an electro-injector for diesel engines and parametric analysis", *SAE Technical Paper Series*, 970349, 1997.
[19] Ficarella, A., Laforgia, D. and Landriscina, V. "Evaluation of instability phenomena in a common rail injection system for high speed diesel engines", *SAE Technical Paper Series*, 1999-01-0192, 1999.
[20] Dongiovanni, C., Coppo, M. "Accurate Modelling of an Injector for Common Rail Systems", Fuel Injection, InTech, ISBN: 978-953-307-116-9, 2010.
[21] von Kunsberg Sarre, C., Kong, S-C. and Reitz, R. D. "Modeling the Effects of Injector Nozzle Geometry on Diesel Sprays", *SAE Technical Paper Series*, 1999-01-0912, 1999.
[22] Vass, S., Németh, H. "Sensitivity analysis of instantaneous fuel injection rate determination for detailed Diesel combustion models", *periodica polytechnica, Transportation Engineering*, vol. 41, no. 1, pp. 77-85, 2013.
[23] Vass S., Zöldy M. "Detailed modeling of the internal processes of an injector for Common Rail Systems", *Journal of KONES Powertrain and Transport*, vol. 25, no. 2, pp. 415-426, 2018.
[24] Kolade, B., Boghosian, M. E., Reddy, P.S. and Gallagher, S. "Development of a General Purpose Thermal- Hydraulic Software and its Application to Fuel Injection Systems", *SAE Technical Paper Series*, 2003-01-0702, 2003.

[25] Vass S., Németh H. “Detailed electromagnetic model of a Common Rail injector”, *34th International Colloquium on Advenced Manufacturing and Repairing Technologies in Vehicle Industry, Visegrád, Hungary*, ISBN 978-963-313-258-6, pp. 165-168., May 2017.

[26] Bárdos, Á., Vass, S., Németh, H. “Validation of a detailed commercial vehicle turbocharged diesel engine model”, *A Jövő Járműve*, vol. 2014, no. 1-2, pp. 25-31, 2014.